CYP3 phylogenomics: evidence for positive selection of *CYP3A4* and *CYP3A7*

Huan Qiu[a], Stefan Taudien[c], Holger Herlyn[b], Juergen Schmitz[d], Yuan Zhou[e], Guopei Chen[e], Roberta Roberto[f], Mariano Rocchi[f], Matthias Platzer[c] and Leszek Wojnowski[a]

Objective **CYP3A metabolizes 50% of currently prescribed drugs and is frequently involved in clinically relevant drug interactions. The understanding of roles and regulations of the individual *CYP3A* genes in pharmacology and physiology is incomplete.**

Methods **Using genomic sequences from 16 species we investigated the evolution of *CYP3* genomic loci over a period of 450 million years.**

Results ***CYP3A*** **genes in amniota evolved from two ancestral *CYP3A* genes. Upon the emergence of eutherian mammals, one of them was lost, whereas, the other acquired a novel genomic environment owing to translocation. In primates, *CYP3A* underwent rapid evolutionary changes involving multiple gene duplications, deletions, pseudogenizations, and gene conversions. The expansion of *CYP3A* in catarrhines (Old World monkeys, great apes, and humans) differed substantially from New World primates (e.g. common marmoset) and strepsirrhines (e.g. galago). We detected two recent episodes of particularly strong positive selection acting on primate *CYP3A* protein-coding sequence: (i) on *CYP3A7* early in hominoid evolution, which was accompanied by a restriction of its hepatic expression to fetal period and (ii) on human *CYP3A4* following the split of the chimpanzee and human lineages. In agreement with these findings, three out of four positively selected amino acids investigated in previous biochemical studies of CYP3A affect the activity and regioselectivity.**

Conclusions **CYP3A7 and CYP3A4 may have acquired catalytic functions especially important for the evolution of hominoids and humans, respectively. *Pharmacogenetics and Genomics* 18:53–66 © 2008 Wolters Kluwer Health | Lippincott Williams & Wilkins.**

Pharmacogenetics and Genomics 2008, **18**:53–66

Keywords: comparative genomics, *CYP3A4*, *CYP3A7*, phylogenomics, positive selection

[a]Department of Pharmacology, Johannes Gutenberg University Mainz, [b]Institute of Anthropology, Johannes Gutenberg University Mainz, Mainz, [c]Genome Analysis, Leibniz Institute for Age Research-Fritz Lipmann Institute, Jena, [d]Institute of Experimental Pathology (ZMBE), University of Muenster, Muenster Germany, [e]Wuhan Botanic Garden, Chinese Academy of Sciences, Wuhan, China and [f]Department of Genetics and Microbiology, University of Bari, Bari, Italy

Correspondence to Professor Dr Med. Leszek Wojnowski, Department of Pharmacology, Johannes Gutenberg University Mainz, Obere Zahlbacher Str. 67, D-55101 Mainz, Germany
Tel: +49 6131 3933460 or 37170; fax: +49 1803 5518 36727;
e-mail: wojnowski@uni-mainz.de

Received 15 June 2007 **Accepted** 8 October 2007

Introduction

CYP3A4, *CYP3A5*, *CYP3A7*, and *CYP3A43* form a gene cluster on human chromosome 7. Protein expression *in vivo* has been demonstrated for CYP3A4, CYP3A5, and CYP3A7. The highest levels of CYP3A proteins are found in the small intestine and in the liver, in agreement with their well-known role in the detoxification of exogenous compounds. The physiological importance of the expression in several other organs, such as prostate and kidney (CYP3A5) or adrenal gland (CYP3A7) is less well understood, except it may involve hydroxylation of steroids and of other physiological compounds. CYP3A4 is the most abundant hepatic CYP3A isoform in adults. CYP3A5 is expressed only in adult carriers of *CYP3A5*1* alleles (~70% Africans, ~30% Asians, and ~10% Central Europeans), in most cases at levels lower than those of CYP3A4. CYP3A7 is the only CYP3A expressed in fetal livers, but it is also found in adult carriers of *CYP3A7*1C* alleles (~15% Central Europeans). *CYP3A43* is considered a pseudogene, based on a low level of mostly aberrant transcripts, although bacteria-expressed protein exhibits some activity [1].

CYP3A metabolizes, at least in part, every second drug currently in use [2]. The reported substrate spectra for CYP3A5 and CYP3A7 are smaller in comparison with CYP3A4, although this judgment is affected to an unknown extent by the variability in the critically important CYP3A expression and reconstitution conditions [1]. CYP3A proteins are frequently involved in clinically relevant drug interactions [2], owing to the combination of their broad substrate spectrum with one or more of the following three factors: (i) pharmacokinetics of CYP3A drug substrates is affected by the largely inherited [3] but unpredictable individual CYP3A4 expression level in the liver and in the small

1744-6872

intestine. This variability may be further enhanced by (ii) CYP3A induction and (iii) inhibition by certain drugs and dietary constituents. The transcription-mediated CYP3A induction, for example, by prescription-free drugs such as St John's wort, may increase the metabolic clearance and attenuate the therapeutic efficacy of a CYP3A substrate [4]. The inducing effects of drugs are mediated by the xenobiotics sensors pregnane X receptor and, to a lesser extent, constitutive androstane receptor. The modulation of CYP3A expression by endogenous compounds is exemplified by the effect of vitamin D, which is mediated by vitamin D receptor [5]. Inhibition, for example, by grapefruit juice has an opposite effect and may increase the concentration of a CYP3A substrate to a toxic level [2].

For all these reasons, a better understanding of CYP3A function and regulation is extremely important both for the development of future drugs and for the safe application of the existing CYP3A drug substrates. Most rapid progress has been achieved in the field of *CYP3A* transcriptional regulation [5]. On the other hand, it is still incompletely understood what makes a drug a CYP3A4 substrate and which gene variants determine the individual CYP3A4 expression level.

Gene function and regulation is increasingly studied using techniques of population genetics and phylogenomics, enabled by the ever-growing number of genome sequencing and genotyping efforts. The evolution of a gene's sequence among human populations, or among species, reflects in part adaptations to changing physiology or environment. We [6] and others [7] recently reported an unusually strong positive selection signal in the *CYP3A* locus in non-African human populations. *CYP3A* loci in these ethnic groups contain low numbers of long-range haplotypes, consistent with their rapid expansion owing to positive selection. Salt–water homeostasis [7] and rickets [6] have been proposed as the underlying selection factors, consistent with the expression of CYP3A5 in the kidney and with the activity of CYP3A4 toward vitamin D, respectively. The identification of selecting factors and genes is notoriously difficult, owing to the confounding impact of population bottlenecks, founder effects, or periods of rapid population expansion [8], but it is medically relevant. Indeed, recent episodes of positive selection frequently represent a response to potentially harmful changes in diet or environment. Some of these factors may be at work today, consistent with the association of *CYP3A* alleles with several current human diseases, notably cancers [9].

Together with *CYP3B*, *3C*, and *3D*, *CYP3A* subfamily belongs to the *CYP3* family, believed to have diverged from other *CYP* genes at least 800 million years ago [10]. *CYP* families are defined by at least 40% amino acid sequence similarity, whereas the corresponding number for subfamilies is 55% [11]. Previous phylogenetic analyses of *CYP3* have been mainly performed on cDNA or protein sequences [12,13]. This had certain unavoidable limitations, as, in addition to true relatedness, similarities among cDNA sequences are strongly affected by species-specific selection and by genomic recombination events. Moreover, owing to limited sampling, *CYP3* evolution in basally diverging amniota and fish-like vertebrates was largely unknown.

Whole genome sequencing of a rapidly increasing number of species makes possible addressing the evolution of gene families by comparative genomic approaches. Using genomic sequences from 16 vertebrate species, we reconstruct in the present work the genomic evolution of *CYP3A* and of the related subfamilies *CYP3B–D* during the last $\sim$450 million years. This is complemented by the investigation of gene conversion events and phylogenetic analysis. Special emphasis was put on the study of $\sim$65 million years of primate *CYP3A* evolution, to facilitate the clarification of the paralogous and orthologous relationships among the *CYP3A* genes in these species. On the basis of this work, we investigated the evolutionary regime that has shaped the contemporary primate *CYP3A* protein-coding sequence, using the ratio of nonsynonymous (amino acid altering) and synonymous (silent) substitution rates ($= d_n/d_s = K_a/K_s = \omega$) as a measure.

Methods and materials

Genomic and cDNA sequences

Genomic assemblies of 16 species were accessed through either University of California Santa Cruz (UCSC) [14] or ENSEMBL (Ensembl is a joint project between EMBL-EBI and the Sanger Institute to develop a software system which produces and maintains automatic annotation on selected eukaryotic genomes) [15] genome browsers or National Center for Biotechnology Information (NCBI) Genbank database. The investigated species were human (*Homo sapiens*, hg18), chimpanzee (*Pan troglodytes*, panTro2), rhesus (*Macaca mulatta*, rheMac2), mouse (*Mus musculus*, mm8), rat (*Rattus norvegicus*, rn4), dog (*Canis familiaris*, canFam2), horse (*Equus caballus*, Equus1.0), opossum (*Monodelphis domestica*, monDom4), platypus (*Ornithorhynchus anatinus*, oaNa5), chicken (*Gallus gallus*, galGal3), frog (*Xenopus tropicalis*, xenTro2), zebrafish (*Danio rerio*, danRer4), fugu (*Takifugu rubripes*, fr1), green spotted pufferfish (*Tetraodon nigroviridis*, tetNeig1), medaka (*Oryzias latipes*, HdrR), and stickleback (*Gasterosteus aculeatus*, gasAcu1). In addition, we analyzed the available partial *CYP3A* locus sequences from olive baboon (*Papio anubis*, Genbank no. AC141417). *CYP3* sequences available from NCBI Genbank and D. Nelson's Cytochrome P450 Homepage (*http://drnelson.utmem.edu/CytochromeP450.html*) were retrieved and mapped in each vertebrate genome by basic local alignment search tool (BLAST).

Partial sequences of the orangutan (*Pongo pygmaeus*) and green anole (*Anolis carolinensis*) *CYP3A* loci were obtained by assembling whole genome shotgun (WGS) sequences. The sequences were obtained by BLAST of known *CYP3A* mRNA sequences to the NCBI trace archive (*http://www.ncbi.nlm.nih.gov/Traces/trace.cgi*). The traces were downloaded, quality clipped, and assembled in GAP4 [16]. All assemblies were manually edited and checked for consistency by distance and orientation of mated-read pairs. In regions not covered by WGS sequences (sequence gaps), the order of contigs was confirmed by at least two mated-read pairs. The genomic assemblies of platypus and baboon *CYP3A* loci (see above) were also checked and confirmed by this approach.

Marmoset (*Callithrix jacchus*) and galago (*Otolemur garnettii*) *CYP3A*-containing bacterial artificial chromosome (BAC) clones were isolated by screening the CHORI-259 and CHORI-256 BAC libraries, respectively (*http://bacpac.chori.org/*). The probe comprised 141-bp *CYP3A* exon 12 sequence amplified from marmoset genomic DNA. Shotgun sequencing of the clones CH259-272B6, CH259-48H24, CH256-186P19, and CH256-241K21 was done using dye terminator chemistry and ABI3730 DNA sequencers (Applied Biosystems, Foster City, California, USA).

cDNA cloning of primate *CYP3A* genes

Liver samples of chimpanzee, orangutan, and rhesus were obtained from Max–Planck Institute for Evolutionary Anthropology, Leipzig, Germany; and liver samples of olive baboon and hamadryas baboon (*Papio anubis*) were obtained from Deutsches Primatenzentrum Göttingen. The RNA was extracted using TRIzol following a standard protocol. Total RNA from the liver of additional rhesus individual was purchased from BioChain Institute, Inc. (Hayward, California, USA). Reverse transcription was performed using SuperScript transcriptase (Invitrogen, Karlsruhe, Germany). Marmoset cDNA was obtained from University of Gottingen, Germany. Primers and PCR conditions of primate *CYP3A* cloning are described in the Supplemental Table S1. The products of reverse transcriptase PCRs (RT-PCRs) were sequenced, either directly or following AT cloning, by GENterprise (Mainz, Germany).

Phylogenetic analysis

One hundred and seven CYP3 amino acid sequences from 31 species were aligned (available upon request) using ClustalX [17] and were manually edited to optimize the alignment. Phylogenetic relationships of these CYP3 sequences were reconstructed using Bayesian and Maximal likelihood methods under JTT + G + I substitution model suggested by Prottest v1.3 [18]. Bayesian inference was performed using program MrBayes [19,20], which estimates posterior probabilities of clade support using Metropolis-coupled Monte Carlo-Markov Chain method (MC^3). The posterior probabilities were estimated using uninformative prior probabilities with inclusion of unequal amino acid frequencies. Two parallel runs, each with four chains, were run for 10 million generations. For each run, three chains were heated and one was cooled with a temperate parameter of 0.20. Rate variation across sites was approximated using a four-category γ distribution and the proportion of invariable sites was estimated from the data assuming a uniform prior distribution. Trees were sampled every 100 generations and following a burn-in of 1000 generations. A 95% majority rule consensus tree was generated to calculate posterior probability values. Maximum likelihood analysis was done using phylogenetic inferences using maximum likelihood (PHYML) [21,22]. The initial tree was determined by neighbor-joining (BIONJ). Rate variation across sites was approximated using a four-category γ distribution. The tree topology, branch lengths, γ-shape parameter, and proportion of invariable sites were optimized by the software during the run. Branch supports were estimated from 1000 PHYML bootstrap replicates.

A rooted phylogenetic tree of 28 primate *CYP3A* genes (Supplemental Fig. S3) was inferred from full-length coding cDNA sequences. Bayesian inference was performed with HKY + G substitution model following the procedure described above for protein sequences analysis. To verify the primate *CYP3A* phylogeny, rare genomic changes (RGCs) were investigated in the 20 *CYP3A* genes (Supplemental Fig. S4) with complete genomic sequences. The sequences were aligned by using Multilimited area global alignment of nucleotide (LAGAN) [23] and shared orthologous intronic retroposed elements and random indels (minimum two nucleotides) were screened as described [24]. The presence/absence of these elements was then mapped on the topology of a sequence-based phylogenetic tree (Supplemental Fig. S4).

Gene conversion

GENECONV program (*http://www.math.wustl.edu/~sawyer/geneconv/*) [25] was used to detect gene conversion events among *CYP3* genes. *CYP3* coding sequences from each species or subfamilies were grouped to form separate datasets. To avoid effects of strong selection and recent mutation, only silent-site polymorphisms were used. The program was run with random-number speed set at 123 for reproducibility. *P* values were computed from 10 000 permutations. The analysis was performed with mismatch not allowed, or with penalty of 1, 2, and 3. Global *P* values lower than 0.05 are considered as evidence for gene conversion. For primate *CYP3A*, additional analysis was also performed on Multi-LAGAN [23] aligned *CYP3A* genomic sequences. The predicted gene conversion events involving short fragments with not enough informative sites were discarded. The redundant events

and false-positive recombination events between genes from different species were filtered out.

Likelihood ratio tests for positive selection

Evolution of primate *CYP3A* sequences was assessed using the ratio of nonsynonymous (amino acid altering) and synonymous (silent) substitution rates ($= dn/ds = Ka/Ks = \omega$) as a measure. As a very conservative estimate, positive (Darwinian) selection ($\omega > 1$) is assumed, if the nonsynonymous substitution rate exceeds the synonymous substitution rate, owing to an overall beneficial effect of amino acid exchanges on individual fitness. An excess of the synonymous substitution rate ($\omega < 1$) indicates negative selection of nonsynonymous substitutions, owing to their detrimental effect on fitness. Finally, neutral evolution ($\omega = 1$) indicates that nonsynonymous substitutions do not affect individual fitness. The analysis was performed using the maximum likelihood approach implemented in phylogenetic analysis by maximum likelihood (PAML) package version 3.15 [26–28]. The analyzed dataset comprised 18 genes from those primate species for which the complete *CYP3A* gene dataset was available (human, chimpanzee, orangutan, and rhesus). The intree used was taken from above phylogenetic analyses. Site-specific and branch-specific analyses were carried out with Codeml. Sites with ambiguity data were not removed from the dataset (cleandata = 0). The codon frequency was estimated from a 3×4 matrix. We performed two parallel likelihood ratio tests (LRTs) for the presence of codon sites with $\omega > 1$ (LRT I + II). A third LRT tested for lineage-specificity of ω (LRT III). For each of the LRTs, twice the log-likelihood difference between alternative and null model was compared with critical values from a χ^2 distribution with degrees of freedom equal to the difference in the number of free parameters between both models (Table 1). LRT I and II compared positive selection model M2a and beta&ω model M8 with the corresponding null models, that is, nearly neutral model M1a and beta null model M7, respectively. To avoid local optima, M8 was run twice with initial ω values smaller or larger than 1. Candidate sites for positive selection were pinpointed using the Bayes empirical Bayes approach. Only sites with a minimum support of 0.95 under M2a or M8 were further considered. LRT III compared free-ratio model and one-ratio model. For details of the implementation of each model, see Refs [26–28]. To pinpoint candidate sites of positive selection along branches of particular interest (Ho7 + Hs4, see Fig. 5), we inferred ancestral sequences using Baseml (model = HKY85, cleandata = 0). Subsequently, we identified nonsynonymous exchanges by pairwise comparison of the sequences at the ends of Ho7 and Hs4, respectively.

Results

Phylogenomics of *CYP3* loci

A total of 25 loci (Fig. 1) containing full-length *CYP3* genes (Supplemental Table S2) were identified in the 16 genomes queried by BLAST with representative *CYP3* sequences from each subclade. *CYP3B*, *C*, and *D* genes were found only in fish species. In most vertebrates, apparently intact *CYP3* genes are located within one of two *CYP3* homologous regions, *CYPHR1* and *CYPHR2*. *CYP3HR1* (*SDK1-CYP3-FOXK1-KIAA0415-FLJ10324*) harbors *CYP3* genes in all non-eutherian vertebrates but frog, tetraodon, and medaka. In Eutheria (placental mammals), *CYP3HR1* contains only *CYP3A* gene remnants (referred to as *CYP3A84P* in D. Nelson's Cytochrome P450 Homepage), whereas all apparently intact *CYP3A* genes are found within the *CYP3HR2* (*CPFS4-ATP5J22-ZNF-CYP3A-OR2AE1-TRIME4-GJE1-AZJP1*). In rodents (rat and mouse), the *Cyp3HR2* got split into two parts by two independent genomic rearrangement events, leading to two *Cyp3a* loci in each species separated by about 8 Mb. The *CYP3HR1* in some fish species contains *CYP3C* or *CYP3D* genes, in stickleback together with *CYP3A* genes. Several additional *CYP3*-containing genomic regions were

Table 1 Test statistics and parameter estimates for the selection in primate *CYP3A* genes

LRTs	Model	*l*	Test statistics	np	Estimates of parameters	Sites with highest support from BEB
LRT I	M1a (nearly neutral)	−5643.60	$2\Delta l = 11.44$ cv = 9.21	2	$P_0 = 0.56$, $P_1 = 0.44$ $\omega_0 = 0.10$, $\omega_1 = 1.00$	–
(site-specific)	M2a (positive selection)	−5637.88	$P < 0.01$	2	$P_0 = 0.60$, $P_1 = 0.33$, $P_2 = 0.07$ $\omega_0 = 0.15$, $\omega_1 = 1.00$, $\omega_2 = 2.63$	Sites with $P_{\omega>1} = 0.87$–0.92: 437, 478, 479
LRT II	M7 (beta)	−5645.72	$2\Delta l = 15.78$ cv = 13.82 $P < 0.001$	2	$P = 0.15$, $q = 0.15$	–
(site-specific)	M8 (beta&ω)	−5637.83		4	$P = 0.50$, $q = 0.80$ $P_0 = 0.89$, $P_1 = 0.11$, $\omega = 2.29$	Sites with $P_{\omega>1} \geq 0.95$: 437, 478, 479
LRT III	M0 (one ratio)	−5692.18	$2\Delta l = 53.06$	1	$\omega = 0.54$	–
(branch-specific)	Free ratio	−5665.65	cv = 46.19 $P < 0.05$	33	See Fig. 5	–

BEB, Bayes empirical Bayes approach; cv, critical value from χ^2 distribution given the difference in the number of free parameters of the models compared; *l*, log likelihood; LRT I, likelihood ratio test for rate heterogeneity; LRT II, likelihood ratio test for the presence of positively selected sites; LRT III, likelihood ratio test for lineage-specificity of ω; np, number of free parameters; $2\Delta l$, twice the log-likelihood difference of the models compared; *P*, level of significance.

Fig. 1

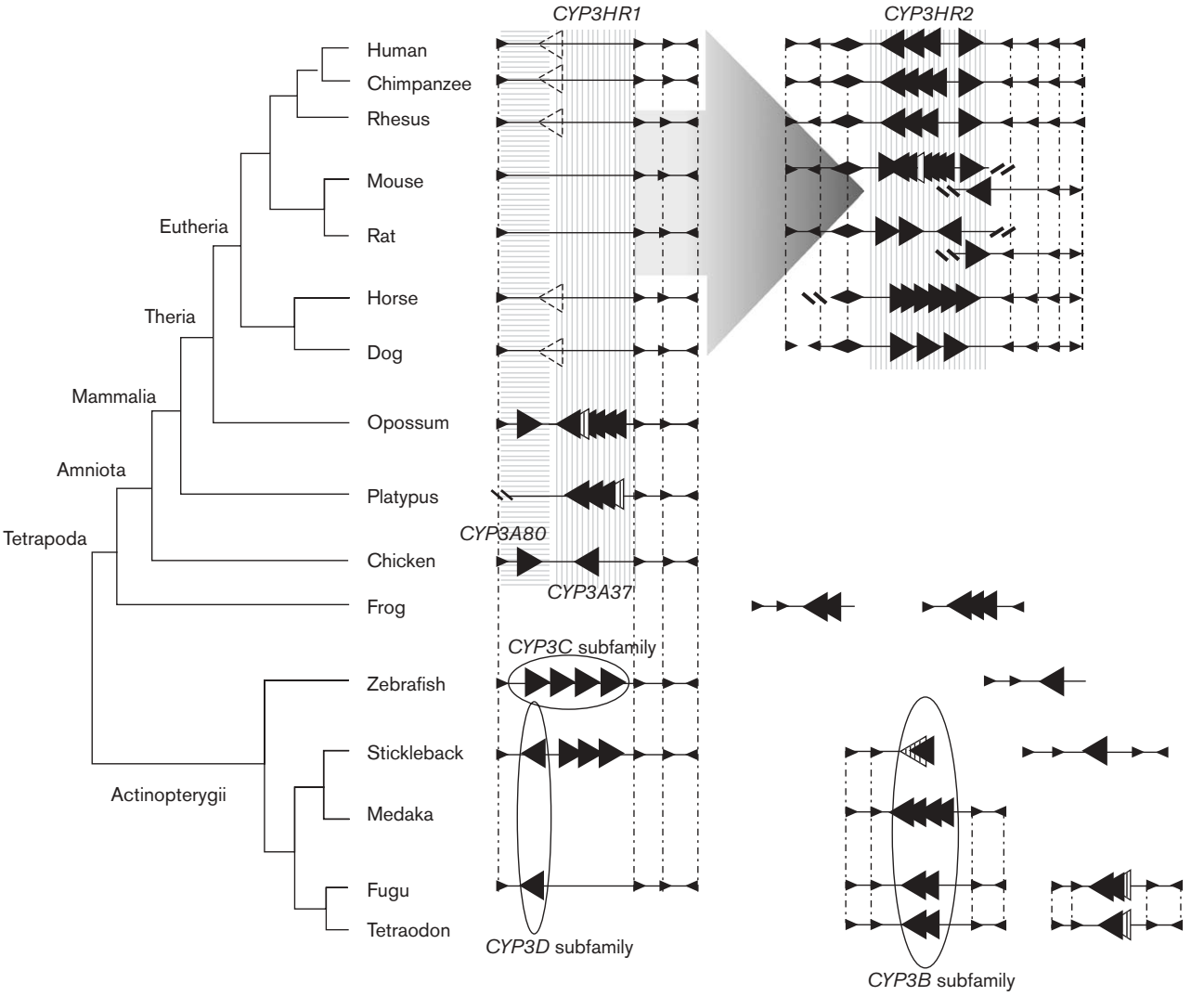

Comparison of *CYP3* loci from 16 different species. Large triangles indicate *CYP3* genes and small triangles indicate flanking genes. Members of *CYP3B*, *CYP3C*, and *CYP3D* subfamilies are circled for easier identification; all other large black triangles are *CYP3A* genes. Remnants of ancient *CYP3A* genes in mammalian *CYP3HR1* (Homology Region 1) are depicted by dashed lines as large transparent triangles. Near-full length *CYP3* pseudogenes are represented by striped triangles. *CYP3A80*-related and *CYP3A37*-related genes found in amniota species are shadowed by grey color in different patterns. The genomic translocation of *CYP3A* from *CYP3HR1* to *CYP3HR2* early in Eutheria evolution is indicated by a large grey arrow. See Supplemental Table S2 for detail information and genomic coordinates of each gene.

found outside *CYPHR1* and *CYPHR2* in the frog and in the fish species (Fig. 1). Thus, the *CYP3B* subfamily is contained in a syntenic region (*KCNH-CYP3B*) in all fish species but zebrafish, whereas all frog *CYP3A* genes were found in two loci specific for amphibians.

Gene conversion

We identified a total of nine potential gene pairs that might have been affected by gene conversion involving the protein-coding regions. These included *CYP3* from rat, dog, pig, medaka, and some primate species (Supplemental Table S3). One of the detected primate gene conversion events replaced exon 6 and a part of intron 6 of *CYP3A7* by the corresponding portion of *CYP3A4* in a common hominidae ancestor, as it is detectable in human, chimpanzee, and orangutan sequences. This is also supported by a 15-bp deletion found in *CYP3A4* and *CYP3A7* genes in these three species, and absent from these genes in rhesus and baboon, and from *CYP3A67* and *CYP3A5* genes in all species (Fig. 2). Moreover, analysis of full-length genomic sequences revealed a number of additional gene conversion events restricted to intron sequences (data not shown).

Fig. 2

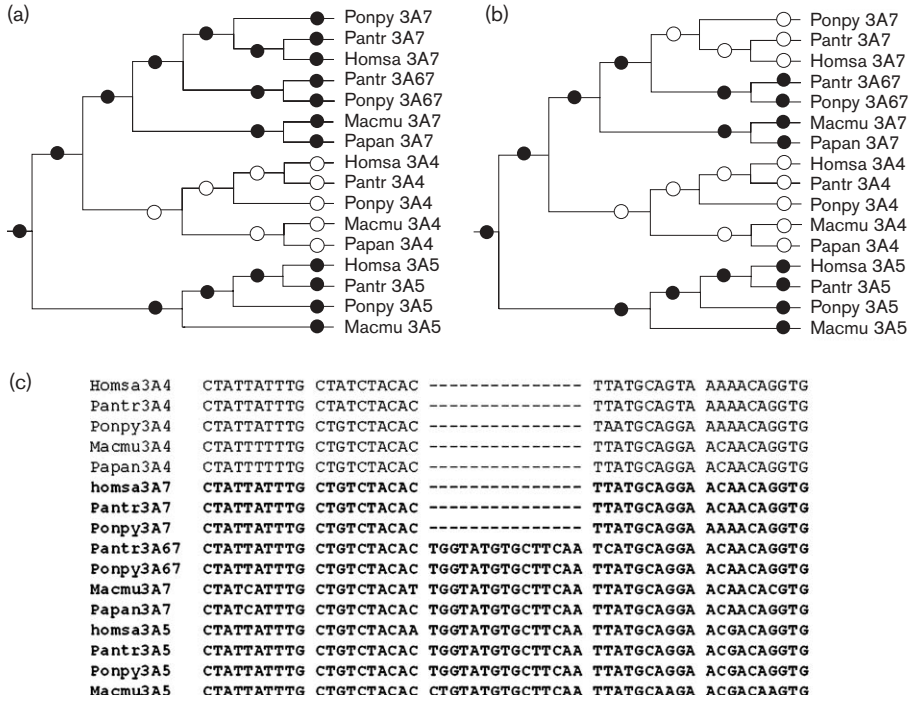

The distribution of the intron 6 15-bp indel among primate *CYP3A* phylogeny, before (a) and after (b) the gene conversion event between hominid *CYP3A4* and *CYP3A7*. The absence and presence of the 15-bp indel is indicated by white and black circles, respectively. (c) The alignment of the indel and the flanking sequences from the *CYP3A* genes studied. Homsa (*Homo sapiens*), Pantr (*Pan troglodytes*), Macmu (*Macaca mulatta*), Ponpy (*Pongo pygmaeus*), and Papan (*Papio anubis*).

Phylogeny of ray-finned fish and amniota *CYP3*

A schematic representation of a phylogenetic tree based on 107 CYP3 protein-coding sequences is given in Fig. 3. The entire tree is provided as a Supplemental Fig. S1. Phylogenetic analysis using Bayesian and maximum likelihood methods produces similar trees, the only difference being the relationships of rodents, primates, and Laurasiatheria *CYP3A* within the well-supported eutherian *CYP3A* clade. We analyzed in more detail fish and non-eutherian amniota, as underrepresented in previous analyses [12,13]. The highest *CYP3* diversity has been achieved in fish species. Examination of the expressed sequence tag (EST) data from several other fish species (Supplemental Table S4) indicates that *CYP3B* and *CYP3C* must have existed at least as early as Percomorpha and Cypriniformes ancestors, respectively. Although the posterior probability and bootstrap support is low (Supplemental Fig. S1), all extant amnioid *CYP3A* genes form two distinct groups (Fig. 3 and Supplemental Fig. S1). The first group ('*CYP3A80* clade' in Fig. 3) includes bird *CYP3A80*, three anolis *CYP3A* genes, all frog *CYP3A*, and one *CYP3A* gene from opossum. The second group ('*CYP3A37* clade' in Fig. 3) comprises bird *Cy3a37*, one anolis *CYP3A*, most *CYP3A* genes from opossum and platypus, and all eutherian *CYP3A* genes. These data together indicate that all extant amniota *CYP3A* genes are derived from two *CYP3A* genes (ancestors of *CYP3A37* and *CYP3A80*) in early amniota. The absence of extant eutherian *CYP3A* in the *CYP3A80* clade suggests that *CYP3A80* orthologs were lost early in Eutheria evolution. Therefore, all *CYP3A* in Eutheria are derived from an ancient *CYP3A37* ortholog.

Genomics and phylogenetics of primate *CYP3A*

Four and five *CYP3A* genes have been reported, respectively, within the human [29] and chimpanzee *CYP3A* loci [13]. We analyzed *CYP3A* loci in three more primate species representing key evolutionary positions in the primate phylogeny: rhesus (Old World monkey), common marmoset (New World monkey), and galago (Strepsirrhini). The rhesus *CYP3A* locus resides on chromosome 3, contains four complete genes (*CYP3A5*, 7, *4*, and *43*), and several pseudogenes composed of detritus exons [11] in an organization resembling that found in the human locus (Fig. 4, see Supplemental Fig. S2 for details). An ~40-kb genomic insertion consisting mainly of low copy number repeats was found between rhesus *CYP3A7* and *CYP3A4*. Sequence analysis of a baboon *CYP3A*-containing BAC (Genbank no. AC141417) revealed a similar insertion between baboon *CYP3A7* and *CYP3A4* genes (data not shown). The marmoset *CYP3A* locus (Genbank accession nos. EF600757

Fig. 3

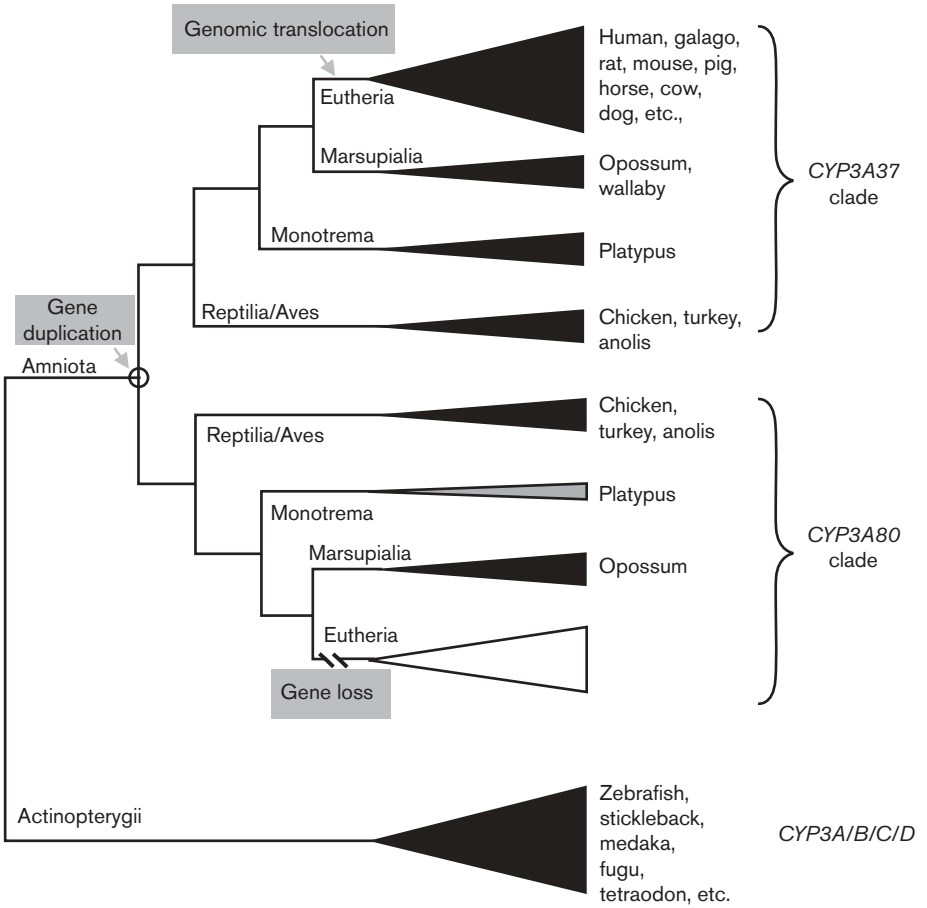

Schematic representation of the *CYP3* phylogeny on the basis of 107 protein sequences from 31 species. Each triangle represents a *CYP3* cluster. Triangle in grey color indicates incomplete sequences not included in tree construction. *CYP3A80*-related genes expected, but not found in Eutheria, are indicated by a white triangle. The animals on right of each triangle represent the taxa from which *CYP3* sequences were used for phylogenetic analysis. For detailed phylogenetic tree, see Supplemental Fig. S1. The major events in amniota ancestor (gene duplication resulting in ancestors of *CYP3A37* and *CYP3A80*), and in eutherian ancestor (genomic translocation of the *CYP3A37* ortholog from *CYP3HR1* to *CYP3HR2* and the loss of *CYP3A80* ancestor), are indicated.

and EF600758) contains three genes (*CYP3A5*, *90*, and *21*) in tandem (Fig. 4). No detritus exons were found in the *CYP3A* intergenic regions. In addition, a processed pseudogene (as evidenced by lack of exon 1 and of all introns, and by multiple in-frame stop codons) related to *CYP3A21* and of unknown genomic location was found by assembling marmoset WGS available through the Trace Archive (data not shown). Galago *CYP3A* locus (Genbank accession nos. EF600755 and EF600756) contains at least three tandem *CYP3A* genes of which one is in the opposite orientation to the others (Fig. 4).

We also examined orangutan *CYP3A*-related WGS data in NCBI Trace Archive. Although the entire structure of orangutan *CYP3A* locus was not obtained, we found the orthologs of all five chimpanzee *CYP3A* genes in this species. All genomic sequence-based in-silico gene predictions of chimpanzee, rhesus, orangutan, and common marmoset *CYP3A* genes were either supported by mRNA sequences in Genbank, or confirmed using reverse transcriptase PCR (RT-PCR) of liver RNA followed by cloning and sequencing (Genbank accession no. EF589790–EF589808). The exceptions were the chimpanzee and orangutan *CYP3A7* genes which, similarly to human *CYP3A7*, might be expressed predominantly prenatally, and galago, liver samples of which were not available. We note that gaps within the *CYP3A* locus in the first release of the chimpanzee genome sequence (panTro1) led to a mix-up between the first exon of *CYP3A67* and the first detritus exon of a *CYP3A* pseudogene in previous publications [13,30].

The reconstructed process of primate *CYP3A* locus evolution shown in Fig. 4 is in agreement with primate

Fig. 4

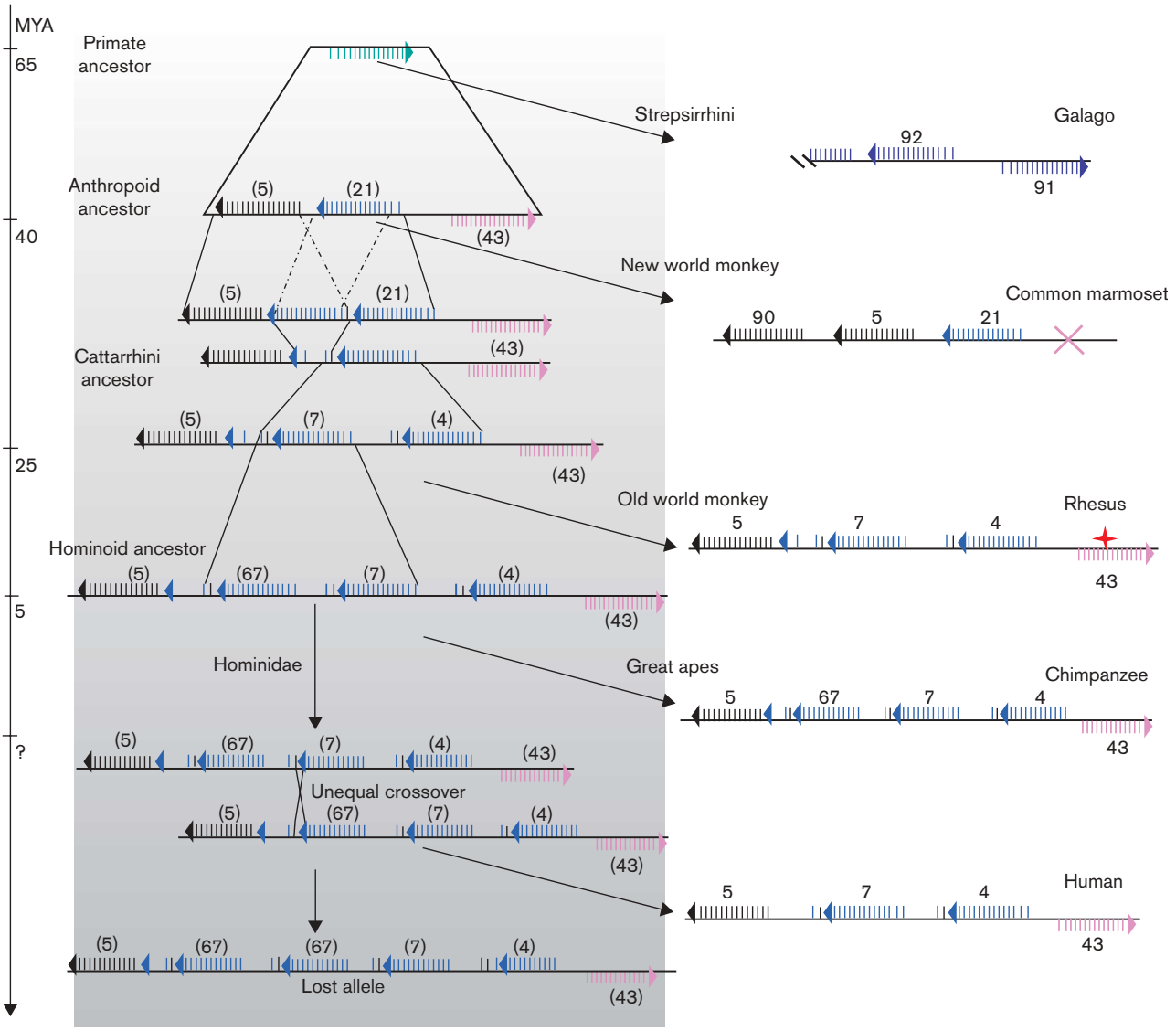

A reconstruction of the evolution of primate *CYP3A* loci. Triangles represent exon 13 in functional *CYP3A* genes or in pseudogenes. Cross represents gene loss in common marmoset. Star represents pseudogenization of rhesus *CYP3A43*. Numbers indicate the gene identity (e.g. 5 = *CYP3A5*). The left part of the figure depicts the ancestral loci, including the apparently lost *5-67-67-7-4-43* allele resulting from the unequal crossover in the human lineage. *CYP3A* loci in selected contemporary primates are shown on the right. Time points of divergence are shown by the *y*-axis on the left (MYA, million years ago).

CYP3A phylogeny (Supplemental Figs. S3 and S4). Galago *CYP3A* resides on the basal position of the primate phylogenetic tree. Marmoset *CYP3A21* shares a common ancestor with catarrhine *CYP3A4*, 7, *67*, and 7, whereas marmoset *CYP3A5* and *CYP3A90* share a common ancestry with catarrhine *CYP3A5*. Human *CYP3A*, *CYP3A4*, *5*, and *43*, each have one-to-one orthologs in all Catarrhine species studied, whereas *CYP3A7* orthologs are restricted to Hominidae. No human *CYP3A* genes have one-to-one orthologs in the marmoset. The primate *CYP3A* phylogeny was strongly supported by orthologous insertion patterns of RGCs (10 retroposed elements and 44 indels) in various loci within primate *CYP3A* genes (Supplemental Fig. S4). Only two conflicting RGCs were found, of which one is covered by the gene conversion shown in Fig. 2.

Evidence for positive selection

According to LRT I and II, the log likelihood value of positive selection model M2a and beta&ω model M8 was significantly higher than the log likelihood value, inferred under assumption, of nearly neutral model M1a and beta-null model M7, respectively (Table 1). Consequently, positive selection can be assumed for single sites of

the 18 catarrhine *CYP3A* genes studied. According to parameter estimates from M2a and M8, about one tenth of sites are under moderate positive selection ($\omega = 2.3$–2.6). Estimates from posterior probability provided significant support of positive selection for codons 437, 478, and 479 ($P_{\omega>1} \geq 0.95$), when taking M8 (Table 1). Though not significant, support from posterior probability was still high for the same sites from M2a ($P_{\omega>1} = 0.87 - 92$). Likewise, the free-ratio model fits the data significantly better than the one-ratio model M0, thus suggesting lineage-specificity of ω (LRT III in Table 1). Out of the 33 branches of the analyzed phylogeny, six branches showed evidence of positive selection (Fig. 5), with the highest ω values for branch Ho7 (*CYP3A7* in the hominoid stem line; $\omega =$ infinite) and Hs4 (human *CYP3A4*; $\omega =$ infinite). The estimated numbers of nonsynonymous changes in Ho7 and Hs4 were 15.5 and 6.0, respectively, whereas the estimate of synonymous codon changes was 0 for either branch. Pairwise comparison of the sequences at the basal and peripheral ends of Ho7 and Hs4 provided similar results. In detail, a total of 18 codon sites were found to show nonsynonymous substitutions along Ho7 (H28R, S29T, V50A, F57Y, F74I, G77C, R78Q, V81M, L108F, S116N, S215P, I220V, S286T, V296M, E333K, A337T, N437S, R484L). The corresponding number for Hs4 was 6 (R54H, R78Q, I129L, I224T, R478S, T489V). The concurrent absence of synonymous exchanges renders these codon site candidates of positive selection along Ho7 and Hs4. Notwithstanding these nonsynonymous exchanges, conservation has played a dominant role in the primate CYP3A evolution. Thus, slight-to-strong negative selection is detected for most sites (89%, Table 1). Moreover, most branches are characterized by ω values less than 1 and, hence, negative selection (Fig. 5).

Fig. 5

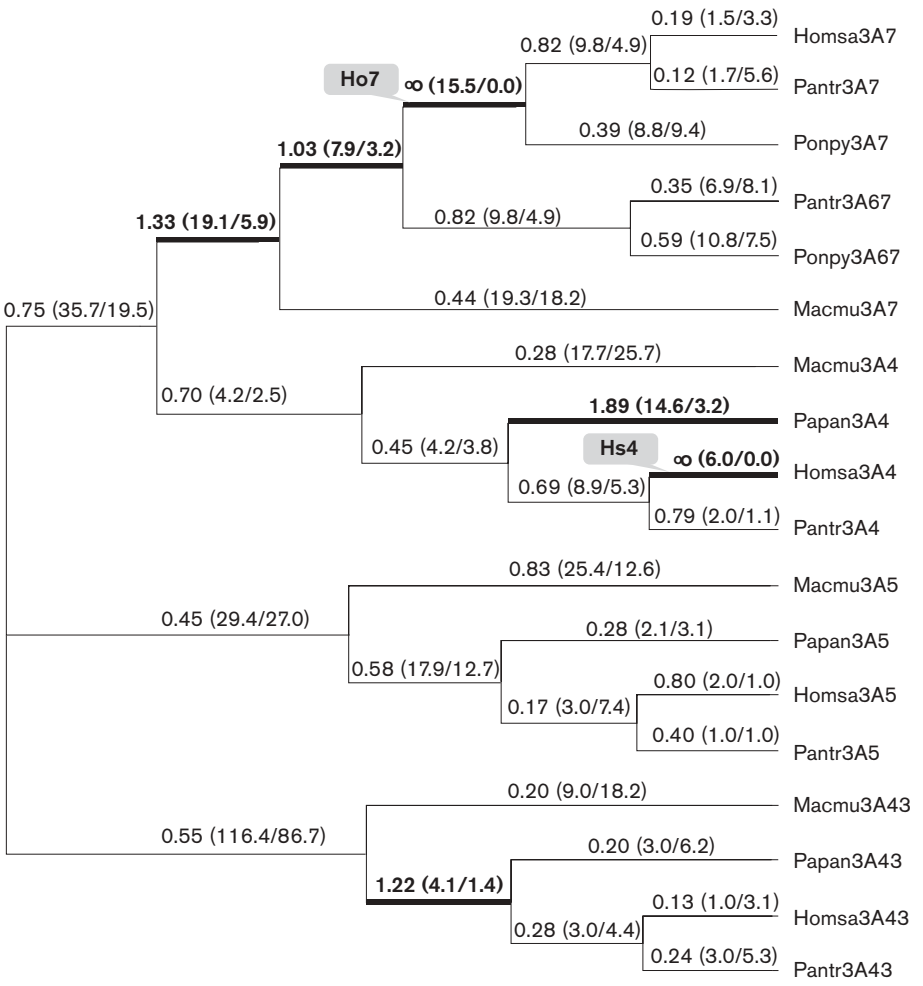

Selection within catarrhine *CYP3A* phylogeny. The branches with ω ratios >1 as estimated by the free-ratio model are shown in thick lines. The estimated numbers of nonsynonymous and synonymous changes are given in the parentheses. Homsa (*Homo sapiens*), Pantr (*Pan troglodytes*), Macmu (*Macaca mulatta*), and Ponpy (*Pongo pygmaeus*).

Discussion

Our combination of comparative genomics, phylogenetics, and selection analysis appears to be a valuable extention of techniques usually applied to investigate enzyme function, such as radiograph analysis, spectroscopic measurements, site-directed mutagenesis, mechanism-based inhibition, and photoaffinity labeling. The last ~450 million years of *CYP3* evolution displays several remarkable features. Most *CYP3* genes of the same clade in the phylogenetic tree build gene clusters within a genomic *CYP3* locus, suggesting a dominant role of tandem duplication in their development. Loci in distantly related species developed through independent gene duplications, despite striking similarities of their structures. In the individual loci, most *CYP3* genes are in a head-to-tail orientation, which confers higher stability of the locus [31]. The oppositely (head-to-head or tail-to-tail) oriented genes, if any, are always the most distantly related, both phylogenetically and physically. In some cases, these genes are located in another subclade of the phylogenetic tree (e.g. opossum *CYP3A80*) or even belong to a different *CYP3* subfamily (stickleback *CYP3D1*). This indicates the common role of inverted duplication in the early expansion of *CYP3* loci.

The highest diversification of *CYP3* has taken place in fish species, which are the only ones containing *CYP3B* through *3D* subfamilies. This is suggestive of a function of *CYP3B–3D* genes in the adaptation to specific aquatic environments, consistent with the expression of *CYP3C1* in the gill and skin of zebrafish [32]. *CYP3* diversification in the fish species was in a few cases independent from their syntenic relationships at genomic level. Although *CYP3HR1* typically harbors *CYP3A* genes, in zebrafish it contains four *CYP3C* genes with organ expression different from *CYP3A* [32]. Conversely, the zebrafish *CYP3A65* is located apart from the *CYP3HR1*. A similar situation is observed in fugu and stickleback *CYP3* genes, in which both *CYP3D* genes are found in *CYP3HR1*.

CYP3A genes from amniota form two distinct groups in the phylogenetic tree ('*CYP3A37*' and '*CYP3A80*' in Fig. 3). We propose that at least two *CYP3A* genes existed in the amniota ancestor before the split of Sauropsida and Mammalia. This is further supported by our comparison of the genomic structure of chicken, opossum, and platypus *CYP3A* loci. Although opossum *CYP3A101–106* and platypus *CYP3A107–109* result from independent duplications of an ancestral *CYP3A37* homolog, the opossum *CYP3A80* gene arose from an ancestral *CYP3A80* homolog.

Upon the emergence of eutherian mammals, the ancestral *CYP3A80* ortholog got lost, whereas, that of *CYP3A37* translocated from *CYP3HR1* to *CYP3HR2*. This has led to a deserted *CYP3HR1*, and to the evolution of *CYP3A* genes in eutherian mammals in an environment different from all other species. Interestingly, except for loss of *CYP3A* genes, eutherian *CYP3HR1* remains remarkably intact, indicating no structural instability. It is tempting to speculate that the novel genomic location, that is, *CYP3HR2*, may have been selected following a rare translocation event from *CYP3HR1* owing to certain fitness advantages. It is known that some genomic locations affect gene expression [33] and protein evolution [34,35]. *CYP3A* is expressed in placenta, where it may play a fetus-protecting role by metabolizing steroids and foreign substrates [36].

Evolution of primate *CYP3A*

Primate *CYP3A* loci appear to have evolved very different in Strepsirrhini and New World monkey compared with Old World monkeys and Hominoidea. The head-to-head orientation of the galago *CYP3A* (*CYP3A91* and *CYP3A92*) resembles that of *CYP3A43* and *CYP3A4* in Catarrhini (Fig. 4). The sister group relationship of Strepsirrhini (i.e. galago) *CYP3A* and all anthropoid *CYP3A* in the reconstructed phylogeny, however, suggests there was only one *CYP3A* gene in their common ancestor, and all extant *CYP3A* in these two taxa arose through independent duplication along each lineage (Supplemental Figs S3 and S4). Contrary to the repeated duplication of *CYP3A21*-like genes (*CYP3A4*, 7, *67*) in catarrhines, platyrrhines (New World monkey) expanded only *CYP3A5*, as evidenced by *CYP3A* locus structure of the marmoset. Evidence of a marmoset *CYP3A43* ortholog was found neither by screening of a genomic BAC library, nor by the extension of the locus assembly based on the sixfold coverage WGS data until the flanking gene *TRIM4* (data not shown). As *CYP3A43* is located on the basal position of anthropoid *CYP3A* phylogeny (Supplemental Figs. S3 and S4), it must have been created prior to the split of catarrhines and platyrrhines, and therefore is likely to be lost in this species. The small size and the relatively easy handling have led to the consideration of marmosets as a better model of human CYP3A pharmacology than rhesus [12,13]. Although *CYP3A21* and *CYP3A4* exhibit similarities in transcriptional regulation [37], the 5′ upstream regions of marmoset *CYP3A5* and *CYP3A90* notably differ from that of human *CYP3A5*, owing to independent retrotransposable element insertions (data not shown). Taken together, with the substantial differences between marmoset and catarrhine *CYP3A* gene sets, these data argue against marmoset being a good primate model of human *CYP3A*. The same is true for Strepsirrhini (i.e. galago), whose *CYP3A* genes evolved even more divergently.

CYP3A67 arose through a duplication of *CYP3A7*, early in the evolution of Hominidae, as it is found both in the chimpanzee and orangutan. Loss of *CYP3A67* is unlikely to be polymorphic in extant human populations, as judged from our negative, PCR-based screen of 99 Central European and 38 African (Bantu) DNA samples

(data not shown). Owing to the large gaps within the *CYP3* locus in the first release of chimpanzee assembly (panTro1), the loss of *CYP3A67* in the human lineage had been thought to have occurred by homologous recombination between *CYP3A67* and the pseudogene *CYP3AP1* [30]. In contrast, our data suggest an unequal crossover with the breakpoints located downstream of *CYP3A7* and *CYP3A67* (Fig. 4 and Supplemental Fig. S5).

Similar to human *CYP3A43* [29,38], chimpanzee *CYP3A43* produces mostly aberrant transcripts (data not shown). In addition, *CYP3A43* is likely to have become a pseudogene in some rhesus populations. The *CYP3A43* sequences in the WGS database of this species contain a point deletion in exon 9 resulting in a frame shift. We found the same deletion in one of the three rhesus samples investigated (data not shown). These observations are consistent with an ongoing pseudogenization of *CYP3A43*, although a protein-independent function [39] cannot be excluded. Owing to the multitude of possible mechanisms, gene loss or pseudogenization are more likely outcomes of a mutation than gain-of-function gene variants [40]. The loss of *CYP3A67* (humans) and *CYP3A43* (marmoset), and the pseudogenization of *CYP3A43* (human, rhesus, and chimpanzee), may therefore represent adaptive responses. On the other hand, the coding region of *CYP3A43* appears to have evolved under strong purifying constraint, as evidenced by the low ω values for the terminal branches leading to these genes (Fig. 5). Taken together, the evolution of primate *CYP3A* was a complex process involving both gene birth and gene death in a lineage-specific manner.

Positive selection and its functional implications

Our analysis of a set of primate *CYP3A* genes revealed a dominant role of purifying (i.e. negative) selection in the primate CYP3A protein evolution, consistent with the conservation of their original biochemical functions. In addition, we detected two episodes of accelerated sequence evolution along branches Ho7 and Hs4. In general, variation of ω among lineages is not considered to be sufficient evidence for adaptive evolution, as it can as well result from relaxation of selective constraint [41]. In case of Ho7 and Hs4 evidence for positive selection, however, is rather strong: first, the ω estimate for Ho7 and Hs4 is infinite, that is as high as it can be. Second, the results from branch-specific analysis (free-ratio model) are supported by pairwise sequence comparison that identified 18 and 6 candidate sites of positive selection along Ho7 and Hs4. Taken together, it appears justified to us to assume positive selection for Ho7 and Hs4, instead of relaxation of selective constraint. The selection of *CYP3A7* took place simultaneously with the origin of Hominoidea, or with the split of this superfamily into Hominidae (human, chimpanzee, gorilla, and orangutan) and Hylobatidae (gibbon). The exact evolutionary branch will be identified only after the cloning of gibbon *CYP3A* genes. Around the same time period, a gene conversion replaced exon 6 of *CYP3A7* with that of *CYP3A4* and *CYP3A7* became a predominantly fetal gene in hominoids. This latter conclusion is based on the absence of *CYP3A7* expression in adult hominids, in contrast to rhesus, olive baboon, and hamadryas baboon. All these events are consistent with a rapid change of an existing one, or with the acquisition of an entirely new function by *CYP3A7*. Strong positive selection acted also on *CYP3A4* following the split from the chimpanzee lineage (branch Hs4, Fig. 5).

Of the 18 amino acids identified as selected in CYP3A7, all but residues 78 and 108 differ between the contemporary human CYP3A4 and CYP3A7 protein sequences. 78Q is also the only amino acid common for CYP3A4 and CYP3A7 out of six residues positively selected in the human CYP3A4. Apparently, 78Q arose from an ancestral R twice, during the independent selection episodes on branches Ho7 and Hs4. This parallel amino acid exchange (R78Q) suggests a particular functional advantage of 78Q, which is at present unknown.

108F is found in both human CYP3A4 and CYP3A7, yet a strong selection signal is detected only in branch Ho7. This apparent contradiction can be explained by the plesiomorph F residue, common for the CYP3A21/CYP3A4/CYP3A7/CYP3A67 group, first changing into 108L within the CYP3A7 lineage and reverting to 108F owing to the selection on Ho7. Together with 215F and five other phenylalanine residues, 108F forms a highly ordered hydrophobic core above the active site of CYP3A4, which may be involved in the initial recognition of substrates or allosteric effectors, or interacts with the electron donors cytochrome b5 or P450 reductase [42]. The identity of the amino acid at position 108 in CYP3A4 affects the activity toward midazolam [43], aflatoxin B1 [44], the steroids testosterone and progesterone [44,45], and lapachole [46]. The importance of the 215P, selected in branch Ho7, for hominoid CYP3A7 proteins, is more difficult to ascertain. Together with amino acids 108 and 120, phenylalanine at position 215 plays a role in the binding and orientation of progesterone in the CYP3A4 active site [47], but its mutagenesis affected neither the activity nor the cooperativity of the enzyme [48,49].

Of the 18 amino acids selected in hominid CYP3A7 (Ho7), eight are located within the first 100 out of 503 amino acids of the protein. This unusual clustering may affect the enzyme's localization to target structures, such as endoplasmic reticulum or mitochondria, which depends on the N terminus. In addition, the N terminus affects the interaction with redox partners such as P450 reductase and cytochrome b5 [45]. In contrast to CYP3A4 and CYP3A5, CYP3A7 has been suggested to be less dependent on b5, although this may be a substrate-specific rather than general feature [50]. The

exact molecular determinants of the reduced interaction with b5 are unknown. The hydrophobic region of the N terminus may also be important for entering of some substrates into the active site [51].

Codons 437, 478, and 479 have been identified as undergoing positive selection across the whole phylogeny. The replacement of the CYP3A4 478S with 478D (like in CYP3A5) had no effect on testosterone hydroxylation, but it reduced the activity by 80–90% and changed the regioselectivity toward aflatoxin B1 metabolites [44]. The substitution of CYP3A4 L479 with T479 (like in CYP3A5) had a similar, reducing effect on the production of the same aflatoxin B1 metabolites. Additionally, it halved the hydroxylase activity of the mutant protein toward testosterone. The mutation of the CYP3A4 479L to 479F (like in CYP3A7) changed the product profile of 7-hexoxycoumarin [52]. The introduction of CYP3A4-derived L at position 479 of the rat Cyp3a9 decreased imipramine N-demethylation and steroid hydroxylation. The latter effect was modified by the identity of the neighboring residue 480 [53]. Taken together, three (108, 478, 479) of the four amino acid residues identified here as positively selected affected the catalytic activity and/or regioselectivity of the enzyme in a complex, substrate-specific manner, when investigated by mutagenesis. The data on residue 215 are less clear.

At present, we can only speculate about the physiological importance of the two, branch-specific positive selection events. Adaptation to global environmental changes is less likely than changes in homeostasis or diet, as both selection events were lineage-specific rather than geographic region-specific. Human CYP3A7 is the only CYP3A expressed in fetal liver and it displays pronounced differences in the metabolism of endogenous substrates, for example testosterone 6β-hydroxylation [54] and DHEAS 16α-hydroxylation [55], compared with CYP3A4, the dominant isoform expressed in the adult liver. The amount of DHEAS in the brain exceeds that in the adrenals, spleen, kidneys, testes, liver, and plasma [56]. Livers of human anencephalic fetuses exhibit extremely low expression of CYP3A7 [57], altogether suggesting a role of CYP3A7-mediated DHEAS metabolism in brain development. Compared with apes, which are mostly herbivorous, humans consumed increasing amounts of animal foods during the last 2 million years [58,59]. The use of fire (i.e. cooking) may have further changed the composition of human diet, which may have accelerated the evolution of human CYP3A4. The resulting changes of the protein sequence may have brought about the wide CYP3A4 substrate spectrum observed in humans. Interestingly, positive selection has been recently detected in the ligand-binding domains of the *CYP3A* regulators pregnane X receptor and constitutive androstane receptor, suggesting adaptation to changing exposure to environmental toxins [60].

Most interestingly, our results allow hypothesizing about the reason for the large interindividual differences in the expression of CYP3A4 observed among contemporary humans. Accelerated protein evolution is accompanied by changes (frequently increases) in the gene's expression levels, as both processes can improve fitness. For example, an increased activity of an enzyme such as CYP3A4 could be brought about through structural changes or by increased expression. Increasing evidence for a coupling between the evolution of protein sequences and their expression levels is found [61,62]. On the other hand, the neutral theory of evolution predicts that the variation in gene expression among individuals of a species increases in parallel to the divergence between species [63]. Taken together, the interindividual variability in CYP3A4 expression in humans may reflect the accelerated evolution of human CYP3A4 protein and its regulatory elements following the split of human and chimpanzee lineages. In agreement with this hypothesis, CYP3A4, which displays the largest interindividual expression variability of all human CYP3A proteins, is the only CYP3A that shows a recent positive selection of its protein sequence. The verification of this hypothesis will require identification of functionally relevant differences in CYP3A4 regulatory elements between humans and chimpanzees.

Acknowledgements

The authors thank Dr Wolfgang Enard (Max–Planck Institute for Evolutionary Anthropology in Leipzig, Germany) for the chimpanzee, orangutan, and rhesus liver samples; Dr Christian Roos (German Primate Center, Göttingen) for olive baboon and hamadryas baboon liver samples; Professor Victor Armstrong (University Göttingen) for common marmoset cDNA; Daniela Werler and Oliver Müller for skillful technical assistance; Markus Schilhabel for bioinformatics support; Professor Hans Zischler (University Mainz) for many useful suggestions throughout the project; and Professor David Nelson (University of Tennessee) for help and comments on sequence data. This work was supported in part by the Deutsche Forschungsgemeinschaft Grant WO505/2-2. The authors acknowledge the support of M.P. and S.T. and L.W. by the Nationales Genomforschungsnetz (NGFN grants 01GR0504 and 01GS0421, respectively).

Supplement data

Supplementary data are available at the *Pharmacogenetics and Genomics* journal online (*www.pharmacogeneticsandgenomics.com*).

References

1 Daly AK. Significance of the minor cytochrome P450 3A isoforms. *Clin Pharmacokinet* 2006; **45**:13–31.
2 Wilkinson GR. Drug metabolism and variability among patients in drug response. *N Engl J Med* 2005; **352**:2211–2221.
3 Ozdemir V, Kalow W, Tang BK, Paterson AD, Walker SE, Endrenyi L, *et al.* Evaluation of the genetic component of variability in CYP3A4 activity: a repeated drug administration method. *Pharmacogenetics* 2000; **10**:373–388.

4 Cvetkovic RS, Goa KL. Lopinavir/ritonavir: a review of its use in the management of HIV infection. *Drugs* 2003; **63**:769–802.
5 Burk O, Wojnowski L. Cytochrome P450 3A and their regulation. *Naunyn Schmiedebergs Arch Pharmacol* 2004; **369**:105–124.
6 Schirmer M, Toliat MR, Haberl M, Suk A, Kamdem LK, Klein K, *et al.* Genetic signature consistent with selection against the CYP3A4*1B allele in non-African populations. *Pharmacogenet Genomics* 2006; **16**:59–71.
7 Thompson EE, Kuttab-Boulos H, Witonsky D, Yang L, Roe BA, Di Rienzo A. CYP3A variation and the evolution of salt-sensitivity variants. *Am J Hum Genet* 2004; **75**:1059–1069.
8 Sabeti PC, Schaffner SF, Fry B, Lohmueller J, Varilly P, Shamovsky O, *et al.* Positive natural selection in the human lineage. *Science* 2006; **312**: 1614–1620.
9 Wojnowski L, Kamdem LK. Clinical implications of CYP3A polymorphisms. *Expert Opin Drug Metab Toxicol* 2006; **2**:171–182.
10 Gonzalez FJ. Molecular genetics of the P-450 superfamily. *Pharmacol Ther* 1990; **45**:1–38.
11 Nelson DR, Zeldin DC, Hoffman SM, Maltais LJ, Wain HM, Nebert DW. Comparison of cytochrome P450 (CYP) genes from the mouse and human genomes, including nomenclature recommendations for genes, pseudogenes and alternative-splice variants. *Pharmacogenetics* 2004; **14**:1–18.
12 McArthur AG, Hegelund T, Cox RL, Stegeman JJ, Liljenberg M, Olsson U, *et al.* Phylogenetic analysis of the cytochrome P450 3 (CYP3) gene family. *J Mol Evol* 2003; **57**:200–211.
13 Williams ET, Rodin AS, Strobel HW. Defining relationships between the known members of the cytochrome P450 3A subfamily, including five putative chimpanzee members. *Mol Phylogenet Evol* 2004; **33**:300–308.
14 Hinrichs AS, Karolchik D, Baertsch R, Barber GP, Bejerano G, Clawson H, *et al.* The UCSC Genome Browser Database: update 2006. *Nucleic Acids Res* 2006; **34**:D590–D598.
15 Hubbard TJ, Aken BL, Beal K, Ballester B, Caccamo M, Chen Y, *et al.* Ensembl 2007. *Nucleic Acids Res* 2007; **35**:D610–D617.
16 Bonfield JK, Smith K, Staden R. A new DNA sequence assembly program. *Nucleic Acids Res* 1995; **23**:4992–4999.
17 Jeanmougin F, Thompson JD, Gouy M, Higgins DG, Gibson TJ. Multiple sequence alignment with Clustal X. *Trends Biochem Sci* 1998; **23**: 403–405.
18 Abascal F, Zardoya R, Posada D. ProtTest: selection of best-fit models of protein evolution. *Bioinformatics* 2005; **21**:2104–2105.
19 Huelsenbeck JP, Ronquist F. MRBAYES: Bayesian inference of phylogenetic trees. *Bioinformatics* 2001; **17**:754–755.
20 Ronquist F, Huelsenbeck JP. MrBayes 3: Bayesian phylogenetic inference under mixed models. *Bioinformatics* 2003; **19**:1572–1574.
21 Guindon S, Lethiec F, Duroux P, Gascuel O. PHYML Online: a web server for fast maximum likelihood-based phylogenetic inference. *Nucleic Acids Res* 2005; **33**:W557–W559.
22 Guindon S, Gascuel O. A simple, fast, and accurate algorithm to estimate large phylogenies by maximum likelihood. *Syst Biol* 2003; **52**:696–704.
23 Brudno M, Do CB, Cooper GM, Kim MF, Davydov E, Green ED, *et al.* LAGAN and Multi-LAGAN: efficient tools for large-scale multiple alignment of genomic DNA. *Genome Res* 2003; **13**:721–731.
24 Kriegs JO, Churakov G, Kiefmann M, Jordan U, Brosius J, Schmitz J. Retroposed elements as archives for the evolutionary history of placental mammals. *PLoS Biol* 2006; **4**:e91.
25 Sawyer S. Statistical tests for detecting gene conversion. *Mol Biol Evol* 1989; **6**:526–538.
26 Yang Z. Likelihood ratio tests for detecting positive selection and application to primate lysozyme evolution. *Mol Biol Evol* 1998; **15**:568–573.
27 Yang Z, Nielsen R, Goldman N, Pedersen AM. Codon-substitution models for heterogeneous selection pressure at amino acid sites. *Genetics* 2000; **155**:431–449.
28 Yang Z, Wong WS, Nielsen R. Bayes empirical bayes inference of amino acid sites under positive selection. *Mol Biol Evol* 2005; **22**:1107–1118.
29 Gellner K, Eiselt R, Hustert E, Arnold H, Koch I, Haberl M, *et al.* Genomic organization of the human CYP3A locus: identification of a new, inducible CYP3A gene. *Pharmacogenetics* 2001; **11**:111–121.
30 Rodriguez-Antona C, Axelson M, Otter C, Rane A, Ingelman-Sundberg M. A novel polymorphic cytochrome P450 formed by splicing of CYP3A7 and the pseudogene CYP3AP1. *J Biol Chem* 2005; **280**:28324–28331.
31 Graham GJ. Tandem genes and clustered genes. *J Theor Biol* 1995; **175**:71–87.
32 Corley-Smith GE, Su HT, Wang-Buhler JL, Tseng HP, Hu CH, Hoang T, *et al.* CYP3C1, the first member of a new cytochrome P450 subfamily found in zebrafish (*Danio rerio*). *Biochem Biophys Res Commun* 2006; **340**: 1039–1046.
33 Verschure PJ. Positioning the genome within the nucleus. *Biol Cell* 2004; **96**:569–577.
34 Pal C, Papp B, Lercher MJ. An integrated view of protein evolution. *Nat Rev Genet* 2006; **7**:337–348.
35 Williams EJ, Hurst LD. The proteins of linked genes evolve at similar rates. *Nature* 2000; **407**:900–903.
36 Hakkola J, Pelkonen O, Pasanen M, Raunio H. Xenobiotic-metabolizing cytochrome P450 enzymes in the human feto-placental unit: role in intrauterine toxicity. *Crit Rev Toxicol* 1998; **28**:35–72.
37 Koehler SC, Von Ahsen N, Schlumbohm C, Asif AR, Goedtel-Armbrust U, Oellerich M, *et al.* Marmoset CYP3A21, a model for human CYP3A4: protein expression and functional characterization of the promoter. *Xenobiotica* 2006; **36**:1210–1226.
38 Domanski TL, Finta C, Halpert JR, Zaphiropoulos PG. cDNA cloning and initial characterization of CYP3A43, a novel human cytochrome P450. *Mol Pharmacol* 2001; **59**:386–392.
39 Hirotsune S, Yoshida N, Chen A, Garrett L, Sugiyama F, Takahashi S, *et al.* An expressed pseudogene regulates the messenger-RNA stability of its homologous coding gene. *Nature* 2003; **423**:91–96.
40 Olson MV. When less is more: gene loss as an engine of evolutionary change. *Am J Hum Genet* 1999; **64**:18–23.
41 Yang Z, Bielawski JP. Statistical methods for detecting molecular adaptation. *Trends Ecol Evol* 2000; **15**:496–503.
42 Williams PA, Cosme J, Vinkovic DM, Ward A, Angove HC, Day PJ, *et al.* Crystal structures of human cytochrome P450 3A4 bound to metyrapone and progesterone. *Science* 2004; **305**:683–686.
43 Khan KK, He YQ, Domanski TL, Halpert JR. Midazolam oxidation by cytochrome P450 3A4 and active-site mutants: an evaluation of multiple binding sites and of the metabolic pathway that leads to enzyme inactivation. *Mol Pharmacol* 2002; **61**:495–506.
44 Wang H, Dick R, Yin H, Licad-Coles E, Kroetz DL, Szklarz G, *et al.* Structure-function relationships of human liver cytochromes P450 3A: aflatoxin B1 metabolism as a probe. *Biochemistry* 1998; **37**: 12536–12545.
45 Domanski TL, Halpert JR. Analysis of mammalian cytochrome P450 structure and function by site-directed mutagenesis. *Curr Drug Metab* 2001; **2**:117–137.
46 Wen B, Doneanu CE, Lampe JN, Roberts AG, Atkins WM, Nelson SD. Probing the CYP3A4 active site by cysteine scanning mutagenesis and photoaffinity labeling. *Arch Biochem Biophys* 2005; **444**:100–111.
47 Park H, Lee S, Suh J. Structural and dynamical basis of broad substrate specificity, catalytic mechanism, and inhibition of cytochrome P450 3A4. *J Am Chem Soc* 2005; **127**:13634–13642.
48 Harlow GR, Halpert JR. Alanine-scanning mutagenesis of a putative substrate recognition site in human cytochrome P450 3A4. Role of residues 210 and 211 in flavonoid activation and substrate specificity. *J Biol Chem* 1997; **272**:5396–5402.
49 Domanski TL, He YA, Khan KK, Roussel F, Wang Q, Halpert JR. Phenylalanine and tryptophan scanning mutagenesis of CYP3A4 substrate recognition site residues and effect on substrate oxidation and cooperativity. *Biochemistry* 2001; **40**:10150–10160.
50 Yamaori S, Yamazaki H, Suzuki A, Yamada A, Tani H, Kamidate T, *et al.* Effects of cytochrome b(5) on drug oxidation activities of human cytochrome P450 (CYP) 3As: similarity of CYP3A5 with CYP3A4 but not CYP3A7. *Biochem Pharmacol* 2003; **66**:2333–2340.
51 Schleinkofer K, Sudarko , Winn PJ, Ludemann SK, Wade RC. Do mammalian cytochrome P450s show multiple ligand access pathways and ligand channelling? *EMBO Rep* 2005; **6**:584–589.
52 Khan KK, Halpert JR. Structure-function analysis of human cytochrome P450 3A4 using 7-alkoxycoumarins as active-site probes. *Arch Biochem Biophys* 2000; **373**:335–345.
53 Xue L, Zgoda VG, Arison B, Almira Correia M. Structure-function relationships of rat liver CYP3A9 to its human liver orthologs: site-directed active site mutagenesis to a progesterone dihydroxylase. *Arch Biochem Biophys* 2003; **409**:113–126.
54 Ohmori S, Nakasa H, Asanome K, Kurose Y, Ishii I, Hosokawa M, *et al.* Differential catalytic properties in metabolism of endogenous and exogenous substrates among CYP3A enzymes expressed in COS-7 cells. *Biochim Biophys Acta* 1998; **1380**:297–304.
55 Kitada M, Kamataki T, Itahashi K, Rikihisa T, Kanakubo Y. P-450 HFLa, a form of cytochrome P-450 purified from human fetal livers, is the 16 alpha-hydroxylase of dehydroepiandrosterone 3-sulfate. *J Biol Chem* 1987; **262**:13534–13537.
56 Leowattana W. DHEAS as a new diagnostic tool. *Clin Chim Acta* 2004; **341**:1–15.

57 Leeder JS, Gaedigk R, Marcucci KA, Gaedigk A, Vyhlidal CA, Schindel BP, *et al*. Variability of CYP3A7 expression in human fetal liver. *J Pharmacol Exp Ther* 2005; **314**:626–635.
58 Milton K. The critical role played by animal source foods in human (Homo) evolution. *J Nutr* 2003; **133**:3886S–3892S.
59 Leonard WR. Food for thought. Dietary change was a driving force in human evolution. *Sci Am* 2002; **287**:106–115.
60 Krasowski MD, Yasuda K, Hagey LR, Schuetz EG. Evolution of the pregnane x receptor: adaptation to cross-species differences in biliary bile salts. *Mol Endocrinol* 2005; **19**:1720–1739.
61 Nuzhdin SV, Wayne ML, Harmon KL, McIntyre LM. Common pattern of evolution of gene expression level and protein sequence in Drosophila. *Mol Biol Evol* 2004; **21**:1308–1317.
62 Lemos B, Bettencourt BR, Meiklejohn CD, Hartl DL. Evolution of proteins and gene expression levels are coupled in Drosophila and are independently associated with mRNA abundance, protein length, and number of protein-protein interactions. *Mol Biol Evol* 2005; **22**: 1345–1354.
63 Khaitovich P, Enard W, Lachmann M, Paabo S. Evolution of primate gene expression. *Nat Rev Genet* 2006; **7**:693–702.